Supplementary Materials for Ultra-thin Van der Waals Magnetic Tunnel Junction Based on Monoatomic Boron Vacancy of Hexagonal Boron Nitride

Halimah Harfah,[1,*] Yusuf Wicaksono,[2,†] Gagus Ketut Sunnardianto,[3,4,5] Muhammad Aziz Majidi,[6] and Koichi Kusakabe[7]

[1] *Graduate School of Engineering Science, Osaka University, 1-3 Machikaneyama-Cho, Toyonaka, Osaka 560-0043, Japan*
[2] *RIKEN Cluster for Pioneering Research (CPR), 2-1 Hirosawa, Wako, Saitama 351-0198, Japan*
[3] *Research Center for Quantum Physics, National Research and Innovation Agency (BRIN), Tangerang Selatan, Banten, 15314, Indonesia*
[4] *Research Collaboration Center for Quantum Technology 2.0, Bandung 40132, Indonesia*
[5] *School of Materials Science and Engineering, Nanyang Technological University, 50 Nanyang Avenue, Singapore 639798, Singapore*
[6] *Department of Physics, Faculty of Mathematics and Natural Sciences, Universitas Indonesia, Kampus UI Depok, Depok 16424, Indonesia.*
[7] *School of Science, Graduate School of Science, University of Hyogo 3-2-1 Kouto, Kamigori-cho, Ako-gun, 678-1297, Hyogo, Japan.*

(Dated: March 1, 2024)

This supplementary material contains additional results that further corroborate the conclusions of the main text and is organized into four sections. Section I discusses the most stable stacking configuration of Cu/hBN/Cu and monoatomic Boron vacancy in hBN(V_B)/Gr/hBN(V_B). Section II provides information on the proximity effect of the Cu electrode surface state on hBN in Cu/hBN/Cu. Section III discusses the transmission probability of pristine Cu and Cu/hBN/Cu as a reference to understand the nature of Cu/hBN(V_B)/Cu transmission probability that is discussed in the main text. Finally, Section IV discusses the charge density distribution and electrostatic potential along the z-axis of Cu/hBN(V_B)/Gr/hBN(V_B)/Cu.

I. Most Stable Stacking Configuration of hBN(V_B)/Gr/hBN(V_B) and Cu/hBN/Cu

Our previous study of Ni/hBN/Gr/hBN/Ni and Quhe et al. of hBN/Gr/hBN, it was found that the most stable configuration between hBN/Gr/hBN was obtained when the N atoms of the upper and lower hBNs at the top and below the hollow site of Gr, while the B atoms were at the top and below the same sublattice C atoms of Gr [1–3]. To confirm whether hBN with monoatomic vacancy (V_B)/Gr/hBN(V_B) has the same most stable stacking configuration, a comparison of the total energy of the selected stacking configurations shown in Figure S1 was performed. The first structure considered is the N atoms of the upper and lower hBN at the top and below the hollow site of Gr, while the B atoms at the top and bottom of the same sublattice C atoms of Gr, which can be written as $NhN - BCB$. The second structure is the N atoms of the upper and lower hBN on the top and below of the C atoms, while the B atoms were on the top and below of the hollow site of Gr, which can be written as $NCN - BhB$. Finally, the third structure is rather similar to the second structure, but the B atoms on the top and below of the another C atoms of the Gr sublattice, which can be written as $NC_AN - BC_BB$. Here, C_A and C_B are the notation for the C atom sublattices A and B of Gr, respectively. Figures S1(a), (b), and (c) shows the structure of the stacking configurations $NhN-BCB$, $NCN-BhB$, and NC_AN-BC_BB, respectively. The total energies for $NhN-BCB$, $NCN-BhB$, and NC_AN-BC_BB are −9614.606929, −9614.303619, and −9613.795601 eV, respectively. The smallest total energy in the stacking of $NhN - BCB$ corresponds to the most stable stacking configuration. This result implies that the monoatomic V_B in hBN does not change the most stable stacking configuration of hBN/Gr/hBN.

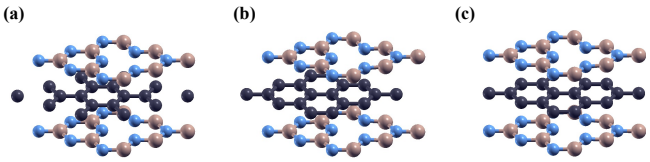

FIG. S1. The stacking of hBN(V_B)/Gr/hBN(V_B) in the (a) $NhN - BCB$, (b) $NCN - BhB$, and (c) $NC_AN - BC_BB$ configurations.

The most stable electrode stacking was also considered when electrodes were attached to hBN(V_B). Since the V_B vacancy does not change the stable configuration of hBN in hBN(V_B)/Gr/hBN(V_B), the most stable configuration of the Cu/hBN(V_B)/Cu interfaces can be obtained considering the most stable configuration of Cu/hBN/Cu. Therefore, three possible stacking configurations between hBN and Cu in Cu/hBN/Cu were considered: 1) Cu atoms placed on top and below of the N atoms of hBN($CuNCu$), 2) Cu atoms placed on top and below of the B atoms of hBN($CuBCu$), and 3) Cu atoms placed on top and below the hollow sites of hBN ($CuhCu$), as shown in Figures S2(a), (b),

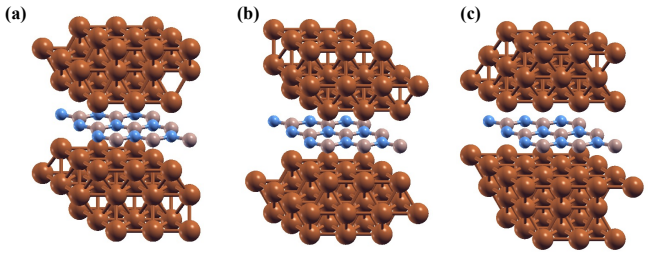

FIG. S2. The stacking of Cu/hBN/Cu in (a) $CuNCu$, (b) $CuBCu$, and (c) $CuhCu$ configurations.

and (c), respectively. The total energies for $CuNCu$, $CuBCu$, and $CuhCu$ are -7745.959208, -7745.810602, and -7745.811920 eV, respectively. The smallest total energy in the stacking of $CuNCu$ corresponds to the most stable stacking configuration. This result means that Cu on top and below the B atoms of hBN(V_B) in the interface between hBN(V_B) and Cu was expected to be the most stable stacking configuration.For Cu/hBN(V_B)/Gr/hBN(V_B)/hBN, the Cu on top and below the B atoms of hBN(V_B) was considered the most stable stacking configuration.

II. The Proximity Effect of the Surface State of the Cu Electrode on hBN in Cu/hBN/Cu

In the most stable stacking configurations, the Cu layer at the interface of Cu/hBN/Cu gives a small but non-negligible proximity effect to the hBN layer, giving a small density of states (DOS) to the insulating gap of hBN as shown in Figure S3(b). The high DOS of the upper and lower Cu at low energy mainly corresponds to the localized state of Cu atoms d-orbital while the broad low DOS from around -1.5 eV to higher energy primarily corresponds to the Cu atoms' s-orbital. The proximity effect comes from the interaction between the s-orbital of Cu near the Fermi energy with p_z-orbital of the N atoms of hBN. The appearance of a small DOS near the Fermi energy on the local density of states (LDOS) of hBN makes the hBN layer a metal. The small DOS of hBN at Fermi energy also leads to possible tunneling transmission through the surface state of Cu atoms's s-orbital

III. Transmission Probability of Pristine Cu and Cu/hBN/Cu

For reference on the spin-polarized electrons transmission in Cu/hBN(V_B)/Cu, the transmission probability of pristine Cu and Cu/hBN/Cu was performed. For the transmission probability of pristine Cu, 18 layers of Cu were considered as scattering regions, with six layers of

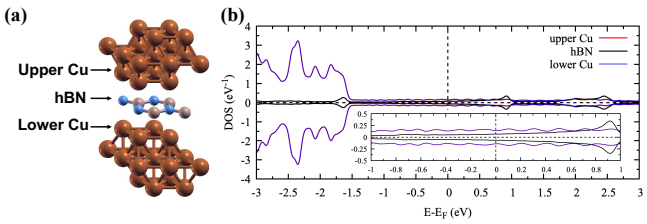

FIG. S3. (a) Cu/hBN/Cu in $CuNCu$ stacking configurations and (b) its local density of states (LDOS) for the upper and lower Cu layers at the interface and the hBN layer.

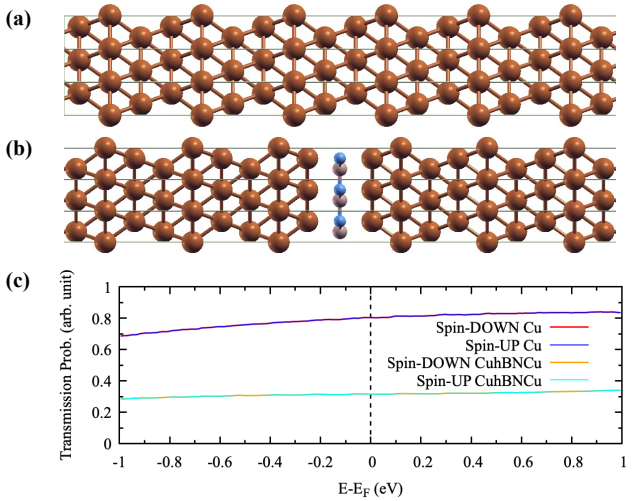

FIG. S4. Transmission probability scattering region setup for (a) Cu pristine and (b) Cu/hBN/Cu. (c)The transmission probability for pristine Cu and Cu/hBN/Cu

Cu used as electrode buffer layers, as shown in Figure S4(a). For Cu/hBN/Cu, a nine-layer Cu/hBN/nine-layer Cu was used as a scattering region with a six-layer Cu on the left and right sides acting as a buffer layer of the right and left electrodes, as shown in Figure S4(b). Figure S4(c) shows the transmission of spin-up and spin-down electrons for pristine Cu and Cu/hBN/Cu. The results show that spin-polarized electron transmission was not observed either case. Furthermore, it also shows that significantly lower electron transmission was observed on Cu/hBN/Cu than observed for pristine Cu.

IV. Charge Density Distribution and Electrostatic Potential of Cu/hBN(V_B)/Gr/hBN(V_B)/Cu

Figures S5(a) and (b) show the planar average charge density distribution along the z-axis direction of the Cu/hBN(V_B)/Gr/hBN(V_B)/Cu system in antiparallel configuration (APC) and parallel configurations (PC). This charge density distribution confirms that no induced magnetic moment created on the Cu layer at the interface and Gr layer due to the magnetic proximity effect of

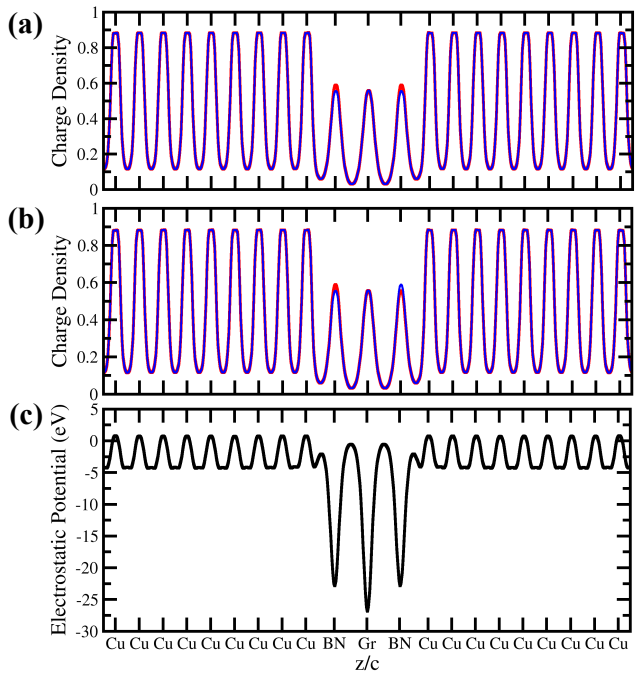

FIG. S5. (a) and (b) Avarage planar charge density distribution along z-axis direction of Cu/hBN(V_B)/Gr/hBN(V_B)/Cu for parallel and anti-parallel configuration, respectively. The red (blue) curve represents spin-up (down) electron density. (c) Average planar electrostatic potential along z-axis direction of Cu/hBN(V_B)/Gr/hBN(V_B)/Cu. The zero energy corresponds to the vacuum level.

hBN(V_B) by looking at the overlap of the spin-up (red curve) and spin-down (blue curve) charge density on the Cu layer at the interface and Gr layer. The different spin-up and spin-down charge densities are only shown on two hBN(V_B) layers. In Figure S5(a), the PC between two hBN(V_B) was considered resulting in a spin-up electron density higher than the spin-down electron density in both hBN(V_B) layers. However, Figure S5(b) shows that the spin-up (down) electron density of the left (right) hBN(V_B) is higher than the spin-down (up) electron density, creating the opposite magnetic moment direction between two hBN(V_B) layers.

In PC and APC, the nonvanishing charge density at the Cu/hBN(V_B) interface is responsible for the electron doping effect on hBN(V_B)/Gr/hBN(V_B). This result can be understood by also examining the planar average electrostatic potential along the z-axis direction of Cu/hBN(V_B)/Gr/hBN(V_B)/Cu shown in Figure S5(c). In the Cu electrode part, a slightly positive electrostatic potential was observed around the nuclei of the Cu atom position, but it became negative when it was removed. This characteristic comes from the metallic nature of the Cu electrode, i.e. delocalization of the valence electrons forms a sea of electrons that move freely throughout the metal lattice. The nonvanishing charge density at the Cu/hBN(V_B) interface corresponds to the nonzero electrostatic potential at the interface, creating electron localization of Cu valence electrons and giving an electron-doped effect.

* harfah.h@opt.mp.es.osaka-u.ac.jp; These authors contributed equally to this work
† These authors contributed equally to this work

[1] R. Quhe, J. Zheng, G. Luo, Q. Liu, R. Qin, J. Zhou, D. Yu, S. Nagase, W.-N. Mei, Z. Gao, and J. Lu, Tunable and sizable band gap of single-layer graphene sandwiched between hexagonal boron nitride, NPG Asia Materials **4**, e6 (2012).
[2] H. Harfah, Y. Wicaksono, G. K. Sunnardianto, M. A. Majidi, and K. Kusakabe, High magnetoresistance of a hexagonal boron nitride–graphene heterostructure-based mtj through excited-electron transmission, Nanoscale Advances **4**, 117 (2022).
[3] Y. Wicaksono, H. Harfah, G. K. Sunnardianto, M. A. Majidi, and K. Kusakabe, Spin-topological electronic valve in ni/hbn–graphene–hbn/ni magnetic junction, Magnetochemistry **9**, 113 (2023).